The uncertainty associated with visual flow fields and their influence on postural sway: Weber's law suffices to explain the nonlinearity of vection

Kunlin Wei

Department of Psychology and Key Laboratory of Machine Perception (Ministry of Education), Peking University, Beijing, China, & Department of Physical Medicine and Rehabilitation, Rehabilitation Institute of Chicago, Northwestern University, Chicago, IL, USA

Ian H. Stevenson

Department of Physical Medicine and Rehabilitation, Rehabilitation Institute of Chicago, Northwestern University, Chicago, IL, USA

Konrad P. Körding

Department of Physical Medicine and Rehabilitation, Rehabilitation Institute of Chicago, Northwestern University, Chicago, IL, USA

When we stand upright, we integrate cues from multiple senses, such as vision and proprioception, to maintain and regulate our vertical posture. How these cues are combined has been the focus of a range of studies. These studies generally measured how subjects deviate from standing upright when confronted with a moving visual stimulus displayed in a virtual environment. Previous research had shown that uncertainty is central in such cue combination problems. Here we wanted to understand, quantitatively, how visual flow fields and uncertainty about them affect human posture. To do so, we combined experimental methods from perceptual psychophysics with methods from motor control studies. We used a two-alternative forced-choice paradigm to measure uncertainty as a function of the magnitude of a random-dot flow field and stimulus coherence. We subsequently measured movement amplitude as a function of visual stimulus parameters. In line with previous research, we find that sensorimotor behavior depends nonlinearly on the stimulus amplitude and, importantly, is affected by uncertainty. We find that this nonlinearity and uncertainty dependence is accurately predicted by standard Bayesian cue combination. Importantly, a Weber's law where visual uncertainty depends on stimulus amplitude is enough to explain the nonlinear behavior.

Introduction

How visual information influences postural control is an intensely studied area of sensorimotor integration. In particular, many studies have shown that postural sway can be elicited by modifying visual stimuli during quiet standing. This paradigm, where the display or virtual environment oscillates to induce self-motion, is usually termed swinging room or moving room (Asten, Gielen, & Gon, 1988; Lee & Aronson, 1974). These studies usually manipulate the velocity, frequency, and amplitude of the visual stimuli to examine how visual cues interact with nonvisual cues, such as vestibular cues or proprioceptive cues, to influence postural sway (e.g., Dijkstra, Schöner, & Gielen, 1994; Keshner, Kenyon, & Langston, 2004; Ohmi, 1996; Peterka, 2002; Soechting & Berthoz, 1979; van der Kooij, Jacobs, Koopman, & van der Helm, 2001). In the present study, we focus on how visual uncertainty impacts postural sway.

Uncertainty is ubiquitous in our sensory and motor systems. There is a growing body of evidence indicating that the nervous system combines sensory cues near optimally for estimation and for movement control (Alais & Burr, 2004; Ernst & Banks, 2002; Ernst & Bülthoff, 2004; Knill & Pouget, 2004; Körding & Wolpert, 2004; Korenberg & Ghahramani, 2002; van Beers, 2009; van Beers, Sittig, & Gon, 1999). For maintaining upright

posture, the nervous system needs to continuously estimate posture and produce muscle commands to regulate this posture. If the nervous system optimally combines the cues from multiple modalities, then visual uncertainty should affect the visually driven postural response. However, the effect of visual uncertainty has not been explicitly addressed; previous studies tended to focus on other features of the visual stimulus and on mechanistic or control-related aspects of sway (Dijkstra et al., 1994; Kuo, 2005; Maurer & Peterka, 2005; Mergner, Schweigart, Maurer, & Blümle, 2005; Morasso, Baratto, Capra, & Spada, 1999; Peterka, 2002; Zacharias & Young, 1981). In the present study, we are, instead, interested in how the postural responses relates to the visual uncertainty in the context of cue combination.

An important finding from previous studies is that induced sway does not continue to increase with increasing stimulus amplitude or frequency of visual stimuli. Rather, postural sway increases and then saturates (Dokka, Kenyon, & Keshner, 2009; Mergner et al., 2005; Peterka & Benolken, 1995; Stevenson, Fernandes, Vilares, Wei, & Kording, 2009; van der Kooij et al., 2001). Researchers usually refer this saturation as a result of sensory reweighting (Jeka et al., 2006; Mergner et al., 2005; Nashner, Black, & Wall, 1982; Oie, Kiemel, & Jeka, 2002; Peterka, 2002). However, a full normative account of this nonlinear relationship between sway and stimulus parameters has not yet been established.

Current theories indicate that this nonlinearity is happening during the process of cue combination (Jeka et al., 2006; Oie et al., 2002; Peterka, 2002), and there have been several interpretations of this nonlinearity. First, it could be that there is a mechanism in place that assigns lower weights to larger amplitudes, potentially as part of a strategy of outlier rejection (Huber, 1964). Alternatively, it could be that the nervous system is integrating signals using Bayes rule and weighting cues by their precision (e.g., Dokka, Kenyon, Keshner, Kording, & Diedrichsen, 2010; Ernst & Banks, 2002). In this case, such nonlinear behavior may emerge from the effects of Weber's law— where the uncertainty increases with stimulus magnitude.

Here we explicitly measured subjects' visual uncertainty to expanding and contracting random-dot flow fields of different velocities and coherence levels using a two-alternative forced-choice task (2AFC). Subsequently, we exposed subjects to the same radial flow fields while they were standing and assessed their postural sway. For the purely perceptual tests, we find that visual uncertainty is an approximately linear function of flow field velocity, in accordance with Weber's law. It is also a function of coherence and the direction of the flow fields. For the motor task, we find that postural sway saturates and declines with increasing velocity of the flow fields, in agreement with previous studies using moving room paradigms. Importantly, these nonlinear responses can be readily explained by a standard Bayesian cue combination model that uses the experimentally observed

visual uncertainty. In other words, the nonlinearity of postural sway as a function of the amplitude of visual stimuli can be understood as simply being the result of Weber's law.

Methods

Subjects participated in three experimental sessions on three consecutive days. Each day, subjects performed a two-alternative forced-choice (2AFC) task as well as a passive standing task. Data were collected from 7 subjects, ages 26–32, 5 males. Two subjects had prior experience in psychophysics experiments and one subject was one of the authors of the paper (KW). All subjects had normal or corrected-to-normal vision and normal balance. All experimental protocols were approved by IRB and in accordance with Northwestern University's policy statement on the use of humans in experiments. Informed consent was obtained from all participants, and subjects were compensated $20 for each day of participation, independent of performance.

Visual stimuli

In both parts of the experiment, subjects were positioned in front of a large projection screen, 60 cm away, and were presented with a random-dot flow field display (Burr & Santoro, 2001; Giaschi, Zwicker, Young, & Bjornson, 2007; Holliday & Meese, 2005; Ptito, Kupers, Faubert, & Gjedde, 2001). The viewable area of the display, 1.55 m × 0.87 m, was intended to cover as much of the field of view as possible (up to approximately 52 deg eccentricity). Subjects were required to wear goggles to minimize visual information in the far periphery, not coming from the display, and were asked to fixate on a central fixation cross, subtending 0.6 deg, throughout the experiment.

The random-dot flow field was composed of 1000 randomly positioned dots moving radially, giving the impression of either expansion or contraction. Each dot had a limited lifetime of 5 frames. Stimuli were presented at a frame rate of 75 Hz, and each dot subtended ∼0.25 deg. Dots that moved off-screen or exceeded their lifetime were repositioned randomly in the viewing area. Perception of optic flow is most affected by peripheral vision, and aliasing at small eccentricities can be a problem. We, therefore, did not display dots within the central foveal region (less than 12 deg eccentricity, see similar treatment, e.g., Dijkstra et al., 1994).

Optic flow was created by radially moving dots—either expansion or contraction. Each dot had a constant local velocity (in pixels/s), and speed did not vary with eccentricity as it would for rigid motion. Although normal postural

sway induces rigid optic flow, nonrigid random-dot motion has the advantage that dot density does not depend on velocity and is constant across velocity conditions. This ensures that dot velocity, rather than dot density, is the primary visual cue. In the sections that follow, we refer to the 10 velocity conditions in screen units (s.u.), which refer to the radial velocity of the dots at an eccentricity of 0 deg (±5, 10, 20, 40, or 80 deg/s). Swing room studies often report stimulus speed in terms of simulated movement in depth rather than radial velocities. For comparison, the radial velocities used here correspond to simulated movement in depth of ±0.32, 0.65, 1.3, 2.5, and 4.8 cm/s at the edge of the annulus (eccentricity of 12 deg). Note, however, that, since the movement is nonrigid, corresponding movement in depth was not constant across the visual field.

We used two uncertainty conditions: 100% coherence, where the dots were not perturbed at all, and 50% coherence, where each dot was manipulated by perturbing the radial position of the dot in each frame with Gaussian noise. In the later case, the noise for each dot and frame was drawn from a Gaussian with a standard deviation of 50% of the normal, unperturbed movement. In the 80 deg/s, 50% coherence condition, for example, each dot moves 7.4 pixels per frame ±3.7 pixels radially.

Assessing visual flow field uncertainty

In the first part of the experiment, subjects were seated in front of the projection screen, with the fixation cross centered at eye level. In a two-alternative forced-choice (2AFC) task, subjects were sequentially presented with two flow fields with the same coherence and slightly different speeds and asked to indicate using a keyboard which field was faster, in terms of absolute speed. Each field was presented as an 800-ms-long motion pulse, and a zero-velocity random-dot flow field was presented between the two stimuli for 200 ms to prevent direct comparison of the fields. This mask consisted of a zero-velocity random-dot field (5-frame lifetime for each dot) and gives the impression of dots randomly appearing and disappearing, without any sensation of optic flow. Following the presentation of the two stimuli, only the fixation cross was shown until subjects responded to report that either the first or second field was faster.

On each trial, the reference random-dot flow field was randomly selected from one of ten velocities (±5, 10, 20, 40, or 80 deg/s at an eccentricity of 0 deg) and was displayed randomly either first or second. Subjects performed 100 trials for each reference field, and the velocity of the test flow field was chosen using optimal experimental design methods (Paninski, 2005). After the first 10 trials, in which the test stimuli were fixed at ±50% of the reference velocity, the next test velocity was chosen to maximize the conditional mutual information between the responses and the parameter for the just noticeable depth difference (JND) given the test velocity. This allowed us to efficiently estimate the JND for each reference velocity and coherence level with relatively few trials. We fitted psychometric functions using an error function (cumulative Gaussian) with fixed mean and assume that there are no lapses in decision making (Whiteley & Sahani, 2008).

Postural responses to random-dot flow fields

In the second part of the experiment, subjects were asked to passively stand in front of the projection screen on a force plate (Nintendo Wii, Balance Board) that was used to measure their center of pressure (COP, Figure 1A). Subjects were instructed to stand comfortably with their feet approximately shoulder width apart, with their arms comfortably at their sides. The projection was moved so that the fixation cross was again centered at eye level. Visual stimuli were the same random-dot flow fields used in the 2AFC task, except instead of sequential presentation followed by a response, subjects were continuously presented with flow fields of varying velocities in pseudorandom order (Figure 3A). Each test stimulus (named motion pulse) was presented for 1.6 s, followed by a rest period lasting randomly between 2.4 and 3.2 s. During this rest period, a random-dot flow field with 0 velocity was displayed. Each of the test stimuli (10 velocities × 2 coherence levels) was presented 30 times resulting in a total of 600 repetitions of motion pulses.

Subjects' COP excursion was recorded continuously at 75 Hz. Since the flow fields were designed to give the impression of optic flow either toward or away from the subject, we are primarily interested in sway along the anterior–posterior axis. For data analysis, the COP data were post-processed by low-pass filtering with a 4th-order Butterworth filter with a cutoff frequency of 10 Hz to remove the measurement noise. To evaluate the postural response, we first aligned individual trials to the stimulus onset and this initial value of COP served as a baseline COP for that trial. Then the integral of COP deviation from the baseline was calculated for each trial and each condition. This alignment and integration of COP captures the effect of the motion pulses and removes most of the low-frequency drift of COP. There are some trials where the COP excursion exhibits excessively large deviation from normal excursions, possibly due to subjects' adjustment of their upper body posture during data acquisition. These trials were identified and removed from further analysis if the COP trajectories fell outside of the median ±15 × std of all COP trajectories for that condition. This resulted in 0.1% to 1.1% of trials excluded for different subjects. Before combining COP measures across subjects, the values from individual subjects were normalized by their own range as inter-subject variance is large due to individual differences in physical properties such as body size.
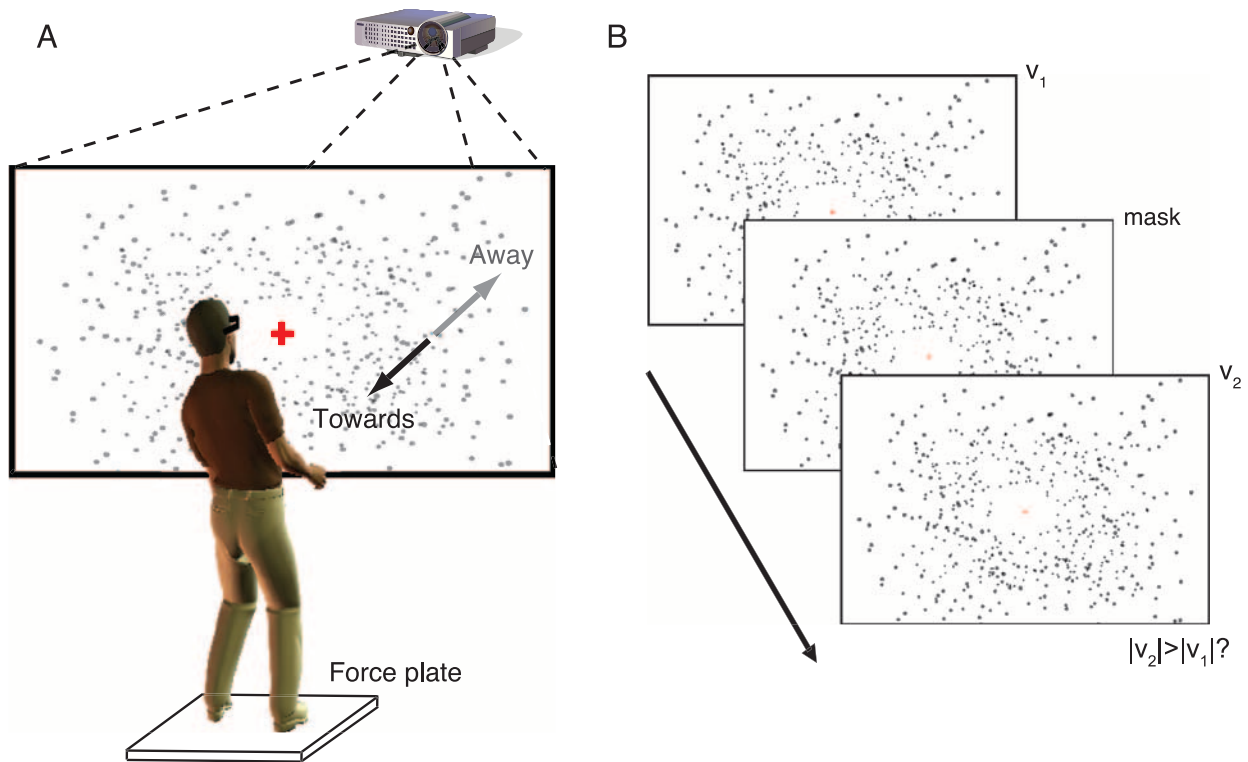
Figure 1. Experimental setup for measuring postural responses to visual stimuli and a schematic of the 2AFC discrimination task. (A) The subject stands on a force plate centered 0.6 m in front of a backprojection screen, on which random-dot flow fields are displayed. The flow field moves toward or away from the subject transiently to elicit anterior–posterior postural sway. (B). During the 2AFC task, two flow field motion pulses are presented with a visual mask in between. Subjects are required to judge whether the second stimulus is faster than the first.

Model

Here we are primarily interested in understanding how subjects integrate visual information from the random-dot flow field with nonvisual (such as proprioceptive and vestibular) cues. We use deviations in the center of pressure as a measure of this perceptual cue combination, and the 2AFC task provides uncertainty measurements for the visual cues. Under the standard optimal cue combination model, cues are combined linearly with weights proportional to their relative precision. Assuming that cues are independent and the prior is noninformative, we say that the probability distribution for the combined, visual–nonvisual estimate of posture is given by

$$p(x|y_{\mathrm{vis}}, y_{\mathrm{nonvis}}) = \frac{1}{Z} p(x|y_{\mathrm{vis}}) p(x|y_{\mathrm{nonvis}})$$

$$= \frac{1}{Z} N(\mu_{\mathrm{vis}}, \sigma_{\mathrm{vis}}) N(\mu_{\mathrm{nonvis}}, \sigma_{\mathrm{nonvis}}), \quad (1)$$

where x is the combined postural estimate, y_{vis} describes the magnitude of the visual cue, and y_{nonvis} describes magnitude of the nonvisual cue. We assume that both the visual and nonvisual cues have Gaussian noise about them. $N(\mu, \sigma)$ denotes a normal distribution with mean μ

and standard deviation σ, and the partition function, Z, ensures that the distribution integrates to 1. We assume that the mean of the visual estimate μ_{vis} is given by the stimulus, with uncertainty σ_{vis} from the 2AFC task. For passive standing, the nonvisual estimate is assumed to have mean 0, and σ_{nonvis} is a free parameter for the uncertainty of the nonvisual cues. The combined estimate of the subject's posture is then given by

$$\hat{x} = \frac{\sigma_{\mathrm{nonvis}}^2}{\sigma_{\mathrm{nonvis}}^2 + \sigma_{\mathrm{vis}}^2} \mu_{\mathrm{vis}}. \quad (2)$$

This 2AFC-calibrated cue combination model has two free parameters: the uncertainty of the nonvisual cues σ_{nonvis} and a linear scaling factor that maps perceptual postural estimates $\hat{x}$ to the observed postural responses. The uncertainty about the visual cues is completely determined by a Weber's law fit to the JNDs estimated during the 2AFC task.

Note that we deliberately avoid describing posture in terms of COP position or velocity. Although a number of studies frame this cue combination problem as a linear feedback control problem where the visual information acts via a multiplicative gain on postural position or velocity, we are primarily interested in the effect of

Weber's law scaling of uncertainty. Both position and velocity should be affected by the scaling of visual uncertainty with velocity, and a number of features of the postural response could be used to measure its effect. Here we use the integral of the anterior–posterior COP deviation in a short time window following presentation of the stimulus. We find this feature of the response to be the most stable.

Results

Visual uncertainty

To predict movement behavior, we need to know the levels of uncertainty associated with all of the radial flow fields. We thus had subjects participate in standard 2AFC tasks where we manipulated the velocity and coherence of the display. Fitting psychometric functions to subjects' judgments in each condition (Figure 2A), we estimated the just noticeable difference (JND) as a function of flow velocity and coherence level (Figure 2B). We find that uncertainty increases with flow speeds in both directions either when the random-dot fields expand or contract, giving the impression of movement toward or away from the screen. This velocity dependency for each direction and coherence level is approximately linear and follows a Weber's law. For the 100% coherence condition, the Weber fractions are estimated at 0.54 ± 0.09 and 0.35 ± 0.05 (mean and *SE* from bootstrapping) for the toward and away conditions, respectively. For the 50% coherence

condition, the Weber fractions are estimated at 0.90 ± 0.05 and 0.57 ± 0.10, respectively. Moreover, flow fields with lower coherence have higher associated visual uncertainty. However, this distinction is not visible for lower speeds and only reached statistical significance for the two largest velocities (paired *t*-test: $p < 0.01$ and $p < 0.005$ for -80 and $+80$ conditions, respectively). The two median velocity conditions (± 40) produce marginally significant difference (both having p around 0.09). This result indicates that the coherence in movement of the random dots can affect the visual uncertainty about speed discrimination of flow field, but its effect is only statistically detectable at large speeds. Lastly, we observed a tendency for subjects' visual uncertainty to be higher when the flow field moved toward the subject in comparison to when it moved away from the subject (left vs. right side of Figure 2B). However, this distinction is significant only for the two largest speeds (± 40 and ± 80, $p < 0.005$).

Postural responses

After measuring the subjects' visual uncertainty for the flow fields, we investigated whether differences in uncertainty can impact postural sway in a systematic way. Subjects were exposed to random-dot flow fields of varying coherence and velocity that were presented in a pseudorandom order (Figure 3A). The velocity change was presented as a pulse change with a duration of 1.6 s, after which the flow field returned to zero speed. Consistent postural responses are difficult to see in the raw COP data (Figure 3A, lower panel). However, if the
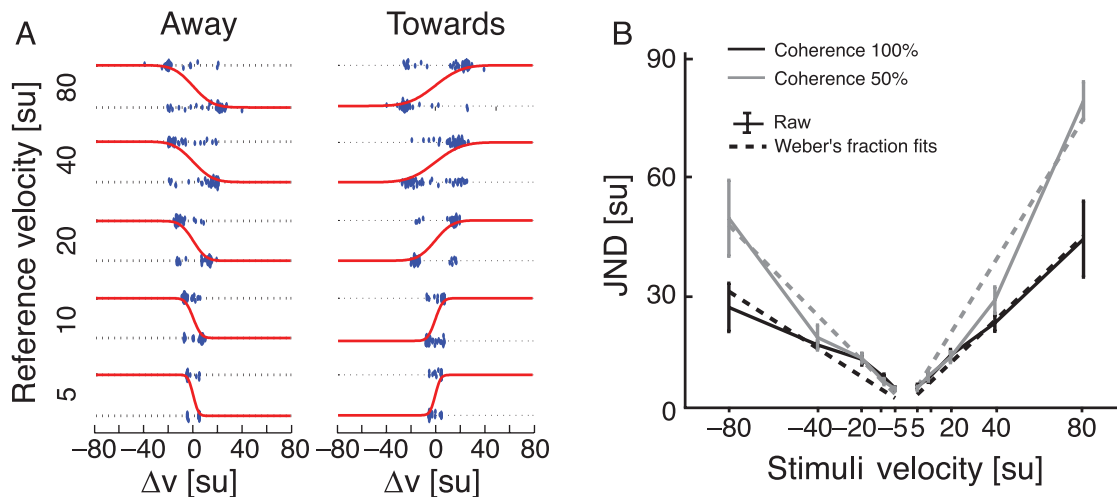

Figure 2. Results from 2AFC tests on visual uncertainty of a radial random-dot flow field. (A) Judgments of whether the second visual stimulus is faster than the first are plotted as a function of their relative velocities; 1 on the *y*-axis stands for a judgment for a faster second stimulus and 0 for a slower one. Individual dots denote individual trials, and the red lines denote fitted psychometric functions. Data are from a typical subject in the 100% coherence condition, with individual panels plotted for different reference flow field velocities. (B) The JNDs derived from 2AFC tests are shown for different conditions. The error bars are subject averages and their *SEM*. The dash lines are fitted linear functions following Weber's law.
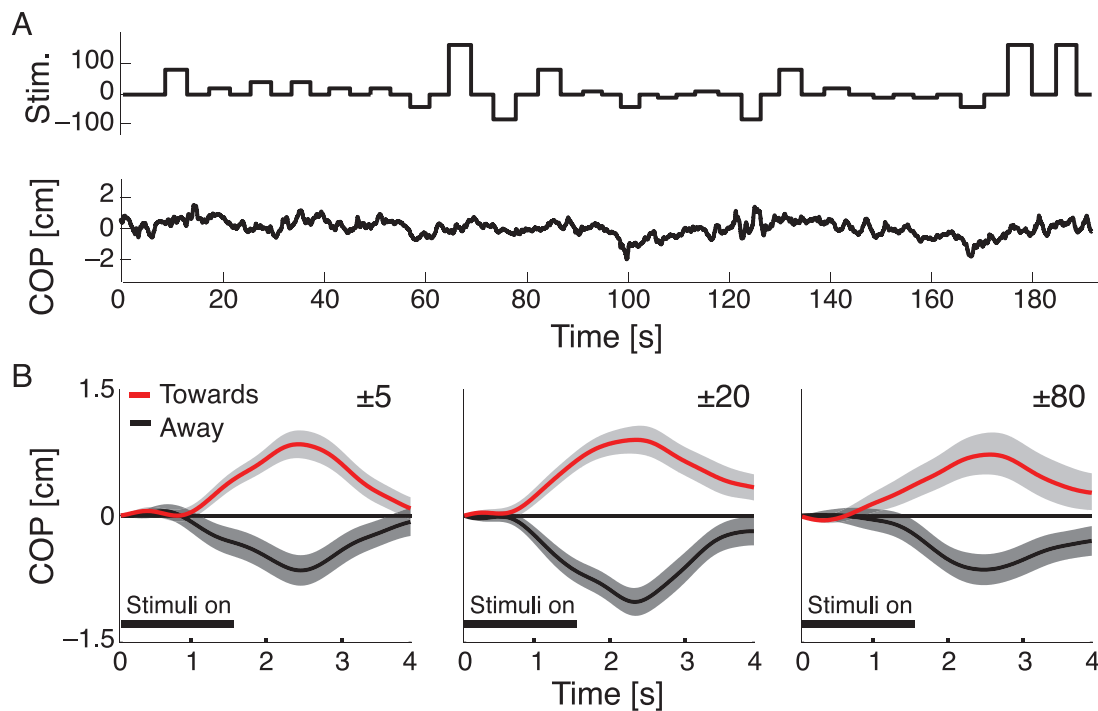
Figure 3. Postural sway data from a typical subject in the 100% coherence condition. (A) A segment of continuous postural data is shown. The upper panel displays the velocity of the radial flow field as a function of time. The lower panel shows the corresponding COP excursion in the anterior–posterior direction. (B) The anterior–posterior COP excursion from the same typical subject for different velocity conditions. Individual trials are aligned to the moment of stimulus onset. The bold lines are the averages across trials in one condition and the shaded regions denote *SEM* across trials. The COP first moves in the same direction as the motion pulse about 1 s after its onset and then returns to the baseline in about 3 s. Comparing across panels, postural sway exhibits a tendency to first increase and then decrease with larger flow field velocity.

COP sequence is triggered to stimulus onset and averaged, the effect of motion pulses becomes clear (Figure 3B). After stimulus onset, the COP starts to move in the direction of visual stimuli. After the motion pulse is turned off, the deviation of COP continues to increase to its maximum and then returns to baseline at about 2–3 s after the motion pulse stimulus is turned off. From the selected velocity conditions, we can also observe that the deviation of COP increases when the flow field velocity increases from ±5 to ±20 s.u. and then decreases as the velocity further increases toward ±80 s.u. These results from a typical subject suggest that the flow field display successfully induced postural sway and that the postural response is a function of flow field velocity.

We can observe systematic effects of flow fields on postural sway (Figure 4, solid). The shape of postural responses as a function of flow field velocity is similar for both coherence conditions: postural sway increases when flow field speed increases from ±5 to about ±20 to ±40 s.u. and then starts to decline. Comparing flow fields moving in opposite directions, it appears that postural sway saturates later when flow fields appear to move toward the subject. Pooling the two coherence conditions together, we compared different velocity conditions. None of the adjacent conditions exhibits a significant difference
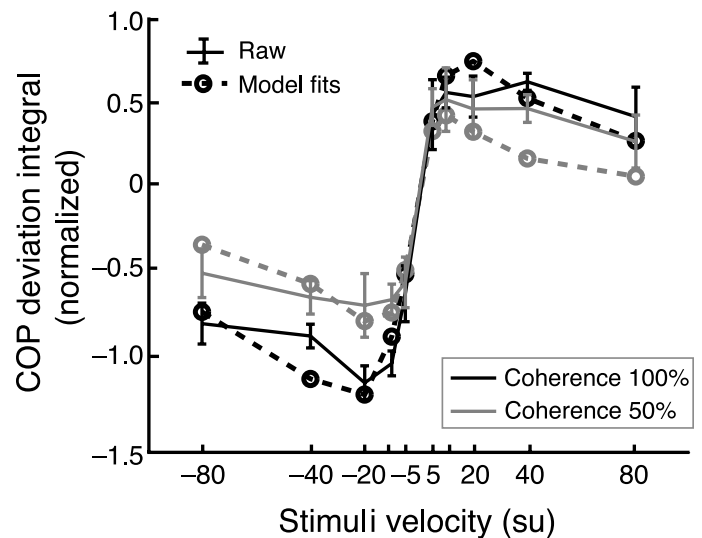

Figure 4. The integral of COP excursion as a function of velocity and coherence of the visual flow fields, as well as the corresponding cue combination model fits. Error bars denote averages and *SEM*s across subjects. Dash lines denote the model fits.

($\alpha = 0.05$) except that +40 condition is significantly larger than +80 condition ($p < 0.05$). Comparing nonadjacent velocity conditions, we found that postural sway in the −20 condition is significantly larger than in −5 condition and −80 condition (paired *t*-test, $p < 0.005$ and <0.05, respectively). If these conditions are compared within coherence conditions, the above comparisons still yield significant differences with one exception: for −20 vs. −80, there is significant difference in 100% coherence case ($p < 0.05$) but only marginally significance in 50% coherence (*p*-value = 0.09). Taken together, these statistical results confirm that the postural sway reached its maximum first with increasing flow velocity and then declined for both directions, though the two maximums are slightly asymmetric in away and toward directions (at −20 and +40, respectively). There is also a tendency that the velocity effect is less pronounced when visual uncertainty is high.

If postural sway (absolute amplitude) is compared between flow field directions, pairwise comparisons between comparable velocity conditions do not find any significant difference except for comparisons between +20 and −20 conditions with 100% coherence, no matter whether the two coherence conditions are pooled or separately treated in the test. However, one-way ANOVA yields significant difference ($p < 0.005$) between directions, indicating that postural sway, on average, is more pronounced with contracting flow fields.

There is a systematic effect of visual uncertainty on postural sway (Figure 4, solid). When data from different velocity conditions are pooled together and submitted to one-way ANOVA, it is found that body sway in 100% coherence condition is significantly larger than 50% coherence ($p < 0.0005$). Within each velocity condition, pairwise comparisons do not find significant differences between two coherence conditions for small velocities (±5, +10, and +20, 4 out of 10 velocity conditions). However, all other comparisons between large velocities return significant results ($p < 0.05$ in general, but $p < 0.005$ for −10 and +40 conditions). Hence, random-dot flow fields of higher coherence, in general, induce larger postural responses, but this effect is mostly pronounced when the optic flow is fast.

Our next question is whether the nonlinear dependency of postural sway on flow field velocity and coherence can be explained by the observations of subjects' visual uncertainty measured during the 2AFC task. Using these measurements, the standard Bayesian cue combination model (see Methods section) has two free parameters: the variance of the nonvisual cue and a linear coefficient that maps perceptual estimates into movement excursions. Using the visual uncertainty values we estimated from fitting Weber's fraction, the model predictions of COP excursion are very close to the actual postural responses (Figure 4, dashed). The nonlinear trend in postural responses is well described by the model predictions; the differences between the two coherence conditions are also reproduced. Overall, the model predictions explain 95.01% of variance in the data. Weber's law is sufficient to explain the nonlinear postural responses that we find during the presentation of random-dot flow fields.

Discussion

To maintain a stable posture, the nervous system needs to incorporate information from multiple senses to accurately estimate the current state of the body and to make appropriate postural adjustments. Using 2AFC psychophysics, we found that for a radial flow field, visual uncertainty increases linearly with the flow velocity in accordance with a Weber's law. We found evidence that flow fields appearing to move toward the subject carry more uncertainty compared to those moving in the opposite direction. The visual uncertainty was also modulated by the coherence level of the flow field. In postural response tests, we found that uncertainty in visual stimuli impacts the upright standing posture in a systematic way. In general, we found that the induced postural sway increased and then declined with increasing flow speeds. Furthermore, postural sway was more pronounced with the high coherence stimuli. Using the visual uncertainty measured during the 2AFC task as inputs, our simple cue combination model predicts the postural responses observed during behavioral tests. Systematic effects of visual uncertainty onto postural sway suggest that regulating upright posture involves a continuous estimation process in which visual and nonvisual cues are combined in a near-optimal manner.

Our findings clearly support the view that multimodal cue combination contributes to the nonlinear effect of visual stimuli on standing posture. This is in line with previous studies that suggested the role of sensory reweighting (Jeka et al., 2006; Kuo, 2005; Mergner et al., 2005; Nashner et al., 1982; Oie et al., 2002; Peterka, 2002; van der Kooij et al., 2001). By measuring the velocity dependence of visual uncertainty, we find clear evidence for a Weber's law type scaling of uncertainty. We provide evidence that the resulting cue combination is achieved in a near-optimal way as prescribed by Bayesian statistics. This finding is in accordance with previous studies that found such scaling in timing tasks where the timing uncertainty is linearly scaled with duration and that also found near-optimal behavior (Hudson, Maloney, & Landy, 2008; Jazayeri & Shadlen, 2010). We argue that sensory reweighting in the context of posture control is a natural result of this optimal estimation in the context of Weber's law: the final estimation of posture will be less influenced by larger stimuli, since they have more uncertainty associated with them. Near-optimal, multimodal cue combination is thus an integral part of postural control (see also Dokka et al., 2010; Kuo, 2005; van der Kooij et al., 2001).

An alternative explanation for the nonlinearity of vection is that the nervous system may perform a more sophisticated type of integration. Several studies have proposed models where the nervous system first determines whether a given cue is relevant and then ignores or reduces the influence of irrelevant or outlying information (Dokka et al., 2010; Wei & Kording, 2009). Under these causal inference or outlier detection models, very rapid visual stimuli are interpreted as movements of the surrounding environment rather than by-products of changes in posture. Whereas the cue combination model used here combines visual and nonvisual cues based on their relative uncertainty, these models weight the cues according to their uncertainty as well as their cause: large stimuli are more likely to come from the environment and thus less relevant for estimating posture. This structured probabilistic account is certainly applicable for the nonlinear effects found in previous studies where visual uncertainty does not vary across stimuli or changes very little. On the other hand, our findings suggest that in situations where uncertainty varies substantially across stimuli, Weber's law may suffice to explain nonlinear behavioral responses.

Our study instead employs flow fields to measure the uncertainty associated with different visual speeds and focuses on testing whether visual uncertainty can bring similar nonlinear postural response. One advantage of our cue combination model is its simplicity: it can explain the same nonlinear effect with less model parameters. Admittedly, outlier detection models might be applicable if the amplitude of visual stimuli increases to the point where cognitive processes to judge whether visual stimuli are relevant for postural estimation become necessary. Nevertheless, we argue that for the slow visual speeds in the current study, simple cue combination with Weber's law suffices to explain the nonlinearity in postural sway.

In contrast to previous studies, here we presented visual stimuli as motion pulses in random-dot flow fields that transiently perturbed the standing posture. The majority of studies in swinging room paradigm used continuous oscillating, structured scenes to drive postural sway (e.g., Asten et al., 1988; Dijkstra et al., 1994; Dokka et al., 2009; Keshner et al., 2004; Lee & Aronson, 1974; Mergner et al., 2005; Ohmi, 1996; Peterka, 2002; Peterka & Benolken, 1995; Soechting & Berthoz, 1979; van der Kooij et al., 2001). As we are primarily interested in the influence of visual uncertainty on postural sway, we used motion pulses to greatly simplify the task and analyses: we can focus on the average effect of visual stimuli instead of full, time-dependent responses. Furthermore, using random-dot flow fields enables us to readily manipulate visual uncertainty by varying the coherence level and to critically test the cue combination hypothesis. Employing motion pulses also makes our investigation more similar to the real-life situation where sudden visual perturbations are frequently encountered.

Our model focuses on the magnitude of the movement of the body and ignores its specific temporal profile. Models that include dynamics and control of the body (Kuo, 2005; van der Kooij et al., 2001) have been shown to be excellent at describing the time course of movement in similar situations. Our estimation model based Weber's law could be readily combined with these models. However, for modeling time-varying sway, it may also be important to incorporate the relevant time scales of different senses (Morasso et al., 1999). Since we are primarily interested in how visual uncertainty modulates postural sway, we simplified the problem by putting all nonvisual cues into a single category and focused on average effect of amplitude.

The linear relationship between visual uncertainty and speed that we find here differs from a previous report of a constant uncertainty over speeds (Stocker & Simoncelli, 2006). However, this previous study used horizontally drifting gratings whereas the present study used expanding/contracting random-dot flow fields. These differences suggest that the uncertainty associated with speed perception depends on the direction of visual stimuli, and also, potentially on the format of the display. Our results indicate that visual perception of speed in radial flow fields follows Weber's law.

Previous motor control studies of standing posture have also found indirect evidence for more visual uncertainty being associated with faster speeds. In these studies, oscillatory visual stimuli were used to induce postural sway and were superimposed on top of translational visual stimuli (Jeka et al., 2006; Ravaioli, Oie, Kiemel, Chiari, & Jeka, 2005). The translational velocity of the visual stimuli has been reported to induce more postural variability (Ravaioli et al., 2005). Furthermore, increasing translational speed appears to produce smaller postural responses (Jeka et al., 2006). These authors proposed that there is more noise in visual stimuli associated with higher translational speeds. However, these findings are not direct tests of visual uncertainty. Furthermore, these studies presented translational (and superimposed) visual stimuli in medial–lateral direction, the direction in which a constant visual uncertainty over speeds was found in psychophysics (Stocker & Simoncelli, 2006). The present study employed standard psychophysics tests to measure the visual uncertainty in the radial flow fields and confirmed that uncertainty of visual stimuli increases with faster velocities.

The asymmetric postural responses for stimuli that appear to move away vs. toward subjects are consistent with previous findings that expansion of optic flow usually evokes larger neural responses than contraction (Gilmore, Hou, Pettet, & Norcia, 2007; Holliday & Meese, 2005; Ptito et al., 2001). Interestingly, we also find an asymmetry in visual uncertainty from the psychophysical tests. Higher visual uncertainty is associated with expanding flow fields, which leads to less postural sway. This

suggests, from yet another angle, that postural sway depends on visual uncertainty.

Uncertainty associated with sensory stimuli depends on the magnitude of the stimuli, such as velocity, size, or force and it also depends on other parameters, such as coherence. The resulting varying uncertainty levels will generally affect cue combination both for perception and for sensorimotor integration. Here we found that an interesting nonlinear effect is accurately explained by simply assuming standard cue combination rules in the context of Weber's law.

Acknowledgments

Commercial relationships: none.
Corresponding author: Kunlin Wei.
Email: wei.kunlin@pku.edu.cn.
Address: Department of Psychology, Peking University, Beijing 100871, China.

References

Alais, D., & Burr, D. (2004). The ventriloquist effect results from near-optimal bimodal integration. *Current Biology, 14,* 257–262.

Asten, W., Gielen, C., & Gon, J. (1988). Postural adjustments induced by simulated motion of differently structured environments. *Experimental Brain Research, 73,* 371–383.

Burr, D., & Santoro, L. (2001). Temporal integration of optic flow, measured by contrast and coherence thresholds. *Vision Research, 41,* 1891–1899.

Dijkstra, T., Schöner, G., & Gielen, C. (1994). Temporal stability of the action–perception cycle for postural control in a moving visual environment. *Experimental Brain Research, 97,* 477–486.

Dokka, K., Kenyon, R., & Keshner, E. (2009). Influence of visual scene velocity on segmental kinematics during stance. *Gait & Posture, 30,* 211–216.

Dokka, K., Kenyon, R., Keshner, E., Kording, K., & Diedrichsen, J. (2010). Self versus environment motion in postural control. *PLoS Computational Biology, 6,* 60–64.

Ernst, M., & Banks, M. (2002). Humans integrate visual and haptic information in a statistically optimal fashion. *Nature, 415,* 429–433.

Ernst, M., & Bülthoff, H. (2004). Merging the senses into a robust percept. *Trends in Cognitive Sciences, 8,* 162–169.

Giaschi, D., Zwicker, A., Young, S., & Bjornson, B. (2007). The role of cortical area V5/MT+ in speed-tuned directional anisotropies in global motion perception. *Vision Research, 47,* 887–898.

Gilmore, R., Hou, C., Pettet, M., & Norcia, A. (2007). Development of cortical responses to optic flow. *Visual Neuroscience, 24,* 845–856.

Holliday, I., & Meese, T. (2005). Neuromagnetic evoked responses to complex motions are greatest for expansion. *International Journal of Psychophysiology, 55,* 145–157.

Huber, P. (1964). Robust estimation of a location parameter. *Annals of Mathematical Statistics, 35,* 73–101.

Hudson, T., Maloney, L., & Landy, M. (2008). Optimal compensation for temporal uncertainty in movement planning. *PLoS Computational Biology, 4,* e1000130.

Jazayeri, M., & Shadlen, M. (2010). Temporal context calibrates interval timing. *Nature Neuroscience, 13,* 1020–1026.

Jeka, J., Allison, L., Saffer, M., Zhang, Y., Carver, S., & Kiemel, T. (2006). Sensory reweighting with translational visual stimuli in young and elderly adults: The role of state-dependent noise. *Experimental Brain Research, 174,* 517–527.

Keshner, E., Kenyon, R., & Langston, J. (2004). Postural responses exhibit multisensory dependencies with discordant visual and support surface motion. *Journal of Vestibular Research, 14,* 307–319.

Knill, D., & Pouget, A. (2004). The Bayesian brain: The role of uncertainty in neural coding and computation. *Trends in Neurosciences, 27,* 712–719.

Körding, K. P., & Wolpert, D. M. (2004). Bayesian integration in sensorimotor learning. *Nature, 427,* 244–247.

Korenberg, A. T., & Ghahramani, Z. (2002). A Bayesian view of motor adaptation. *Current Psychology of Cognition, 21,* 537–564.

Kuo, A. D. (2005). An optimal state estimation model of sensory integration in human postural balance. *Journal of Neural Engineering, 2,* S235–S249.

Lee, D., & Aronson, E. (1974). Visual proprioceptive control of standing in human infants. *Perception & Psychophysics, 15,* 529–532.

Maurer, C., & Peterka, R. (2005). A new interpretation of spontaneous sway measures based on a simple model of human postural control. *Journal of Neurophysiology, 93,* 189.

Mergner, T., Schweigart, G., Maurer, C., & Blümle, A. (2005). Human postural responses to motion of real and virtual visual environments under different support base conditions. *Experimental Brain Research, 167,* 535–556.

Morasso, P., Baratto, L., Capra, R., & Spada, G. (1999). Internal models in the control of posture. *Neural Networks, 12,* 1173–1180.

Nashner, L., Black, F., & Wall, C. (1982). Adaptation to altered support and visual conditions during stance: Patients with vestibular deficits. *Journal of Neuroscience, 2,* 536.

Ohmi, M. (1996). Egocentric perception through interaction among many sensory systems. *Cognitive Brain Research, 5,* 87–96.

Oie, K., Kiemel, T., & Jeka, J. (2002). Multisensory fusion: Simultaneous re-weighting of vision and touch for the control of human posture. *Cognitive Brain Research, 14,* 164–176.

Paninski, L. (2005). Asymptotic theory of information-theoretic experimental design. *Neural Computation, 17,* 1480–1507.

Peterka, R. (2002). Sensorimotor integration in human postural control. *Journal of Neurophysiology, 88,* 1097.

Peterka, R., & Benolken, M. (1995). Role of somatosensory and vestibular cues in attenuating visually induced human postural sway. *Experimental Brain Research, 105,* 101–110.

Ptito, M., Kupers, R., Faubert, J., & Gjedde, A. (2001). Cortical representation of inward and outward radial motion in man. *Neuroimage, 14,* 1409–1415.

Ravaioli, E., Oie, K., Kiemel, T., Chiari, L., & Jeka, J. (2005). Nonlinear postural control in response to visual translation. *Experimental Brain Research, 160,* 450–459.

Soechting, J., & Berthoz, A. (1979). Dynamic role of vision in the control of posture in man. *Experimental Brain Research, 36,* 551–561.

Stevenson, I., Fernandes, H., Vilares, I., Wei, K., & Kording, K. (2009). Bayesian integration and nonlinear feedback control in a full-body motor task. *PLoS Computational Biology, 5,* 150–158.

Stocker, A., & Simoncelli, E. (2006). Noise characteristics and prior expectations in human visual speed perception. *Nature Neuroscience, 9,* 578–585.

van Beers, R. J. (2009). Motor learning is optimally tuned to the properties of motor noise. *Neuron, 63,* 406–417.

van Beers, R. J., Sittig, A. C., & Gon, J. J. (1999). Integration of proprioceptive and visual position-information: An experimentally supported model. *Journal of Neurophysiology, 81,* 1355–1364.

van der Kooij, H., Jacobs, R., Koopman, B., & van der Helm, F. (2001). An adaptive model of sensory integration in a dynamic environment applied to human stance control. *Biological Cybernetics, 84,* 103–115.

Wei, K., & Kording, K. (2009). Relevance of error: What drives motor adaptation? *Journal of Neurophysiology, 101,* 655–664.

Whiteley, L., & Sahani, M. (2008). Implicit knowledge of visual uncertainty guides decisions with asymmetric outcomes. *Journal of Vision, 8*(3):2, 1–15, http://www.journalofvision.org/content/8/3/2, doi:10.1167/8.3.2. [PubMed] [Article]

Zacharias, G., & Young, L. (1981). Influence of combined visual and vestibular cues on human perception and control of horizontal rotation. *Experimental Brain Research, 41,* 159–171.